Interfacial Friction-Related Phenomena in Continuous Casting with Mold Slags

Ya Meng and Brian G. Thomas
University of Illinois at Urbana-Champaign
Department of Mechanical and Industrial Engineering,
1206 West Green Street,
Urbana, IL USA 61801
Ph: 217-333-6919; Fax: 217-244-6534
Email: yameng@uiuc.edu, bgthomas@uiuc.edu

Key Words: Continuous casting, Transient model, Heat transfer, Interfacial gap, Mold friction, Mold slag fracture, Oscillation

INTRODUCTION

Many phenomena in continuous casting including the formation of surface defects are greatly affected by heat transfer in the mold[1]. The interfacial slag layers between the solidifying steel shell and the mold wall dominates the resistance to heat removal and thus controls mold heat transfer[2]. Surface defects, such as longitudinal cracks and star cracks have been associated with variation of slag lubrication[3, 4]. High meniscus heat transfer and variation in meniscus heat transfer mechanisms correlate with increased sliver defects, but the reasons are not understood. Thus, improved understanding of slag layer behavior is important for steel quality.

In continuous casting, mold powder is added to the free surface of the liquid steel. It sinters and melts, spreading over the liquid steel surface according to the steel surface contour and flow pattern[5]. During each oscillation stroke, liquid slag is pumped from the meniscus into the gap between the steel shell and the mold wall[6], where it acts as a lubricant, so long as it remains liquid. A solid slag layer forms against the mold wall. Its thickness increases greatly just above the meniscus, where it is called the slag rim. Depending on the composition and cooling rate of the mold slag, the microstructure of the multiple layers that form may be glassy, crystalline or mixtures of both[7]. Figure 1 shows a typical schematic of this region of the continuous casting process.

A substantial fraction of the slag consumed in the mold is entrapped in oscillation marks moving down at the casting speed. When a solid layer stably attaches to the mold wall, the remaining slag consumed is from the flowing liquid layer and is here called "lubrication consumption".

The hydrostatic or "ferrostatic" pressure of the molten steel pushes the unsupported steel shell against the mold walls, causing friction between the steel shell and the oscillating mold wall. At the corners, the shell shrinks away to form a gap, so friction is negligible. Another significant source of friction is at the bottom of the narrow faces, if excessive taper generates friction by squeezing the wide face shell. Finally, misalignment of the mold and strand can cause friction, especially if the stroke is large. It has been proposed that friction may impede increased casting speed[8]. We believe that friction may also cause fracturing of the solidified slag layer that produces local heat flux variation. The accompanying temperature and stress variations in the steel shell

lead to quality problems, such as shear tearing, sticking and even breakouts[9]. Ozgu[10] and Geist[11] both report "saw-tooth" shape temperature fluctuations low in the mold, which suggests solid slag layer fracture and sheeting from the mold wall. Currently mold friction measurements are evaluated usually as a means to detect problems with the oscillation system, such as mold misalignment. If the friction signal can be better understood, friction monitor could be used to identify the condition of mold lubrication, predict surface defects and help to prevent breakout.

Figure 2(a) shows a near 20cm piece of slag film taken from the corner of an operating caster mold. Most researchers believe that a glassy slag layer forms against the mold wall due to high cooling rates during initial contact of the molten slag with the water-cooled copper mold. A liquid layer is present when the shell surface temperature is higher than the slag solidification temperature. Between these two layers, a crystalline layer is expected, according to the time-temperature transformation (TTT) diagram, which has been measured in controlled laboratory conditions[12]. However,

Fig. 1: Schematic of interfacial gap phenomena in continuous casting mold

slag film samples taken form mold wall usually show a different microstructure: a crystalline layer on the mold side and glassy layer on the shell side[13], as shown in Fig. 2(b). Perhaps the glassy layer devitrifies during the long period when solid layer attaches to the mold wall[14] and perhaps the steel side glassy layer forms from quenching liquid slag during obtaining the sample.
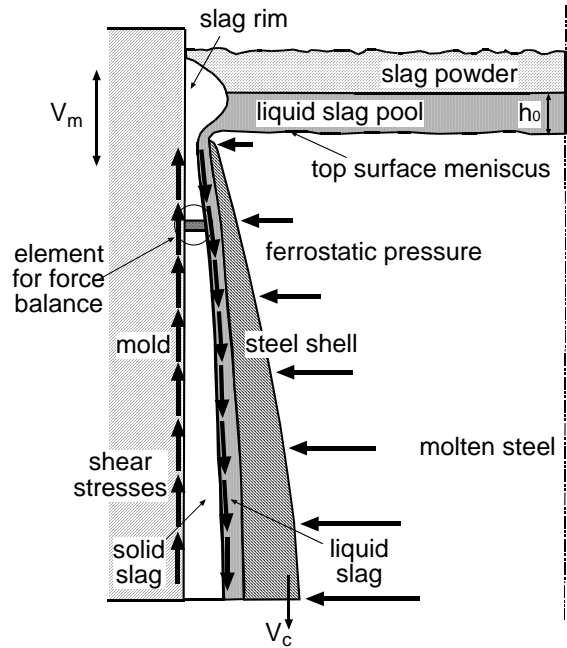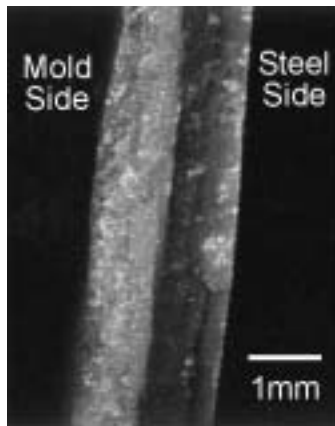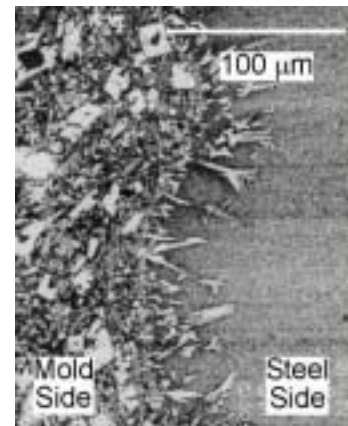

(a) macroscopic film including corner

(b) crystalline and glassy layers

(c) close-up of the crystalline layer growing into glassy layer

Fig. 2: Sample of slag layer and microstructure

Therefore, it is necessary to study the transport of molten/re-solidified slag layers in the interface. A previous paper[15] has discussed steel solidification and heat transfer models of continuous casting. Only a few models have detailed treatment of interfacial layers. Of these, most assume a linear velocity distribution through the liquid film thickness[8, 16]. Several previous models have attempted to quantify gap flow by solving a Navier-Stokes equation[17-21]. In these models, the slag layer thickness either is an input constant[17, 18, 21] or assumed to equal the shrinkage of steel shell[19, 20]. This ignores important phenomena such as ferrostatic pressure. Most previous models assume constant slag viscosity in the gap, which is contrary to the tremendous temperature dependency reported in measurements[22, 23]. Some researchers use a simple inverse function of temperature[20] or fitted Arrhenius equation[21] first given by Riboud[24]. However, the slag viscosity is only measured above the

slag liquidus and is much lower on the mold side. Seldom have models discussed the effect of oscillation marks on lubrication and consumption. Moreover, no previous model describes the solid layer fracture and sliding behavior. Thus, a more comprehensive model of interfacial gap lubrication and heat transfer is needed.

INTERFACIAL MODEL DESCRIPTION AND VALIDATION

The present work models heat transfer, liquid flow and friction in the interfacial slag layers during an oscillation cycle. An analytical solution of the 2D momentum equation is derived for a temperature-dependent viscosity in the liquid slag layer. The model is validated through comparison with a numerical solution, based on heat transfer calculated for typical casting conditions. Shear stress in the liquid slag layer is based on the velocity gradient and liquid viscosity. Next, axial stress and friction in the solid slag layer is obtained by solving a force balance equation. This model is validated using ANSYS. Finally, the program with combined heat transfer, liquid flow and solid friction models, CON1D, is applied to predict typical behavior and critical conditions for fracture and sliding of the interfacial slag layers.

Heat Transfer Model

A simple but comprehensive model of heat transfer in continuous cast steel, CON1D, is used for the current study. The model includes a 1-D transient finite-difference calculation of heat conduction in the solidifying steel shell coupled with 2-D steady-state heat conduction in the mold wall. It features a detailed treatment of the interfacial gap between the shell and the mold, including mass, momentum and force balances on the slag layers and the effect of oscillation marks. Details of this model are presented elsewhere[15].

Liquid Slag Layer Flow Model

For simplicity, the slag is treated as two layers with variable thickness in the vertical (z-) direction: a rigid solid layer and a laminar liquid layer with temperature dependent viscosity.

The following Navier-Stokes equation characterizes the laminar viscous flow of liquid slag vertically within the gap as gravity and downward viscous drag by the steel shell must balance the upward squeezing from the ferrostatic pressure:

$$\rho \cdot \frac{\partial V_z}{\partial t} = \frac{\partial \tau_{xz}}{\partial x} + \left(\rho - \rho_{steel} \right) g \qquad [1]$$

where, x: distance from slag solid/liquid interface; ρ: slag density; ρ_{steel}: steel density.

Shear stress in the liquid slag layer depends on the velocity gradient at each point across the channel:

$$\tau_{xz} = \mu \frac{\partial V_z}{\partial x} \qquad [2]$$

where, μ: slag viscosity.

The temperature dependent viscosity of the liquid slag is fitted to a simple power-law relation, which better estimates low-temperature high-viscosity than a simple Arrhenius equation:

$$\mu = \mu_s \left(\frac{T_s - T_{sol}}{T - T_{sol}} \right)^n \qquad [3]$$

where, μ_s: slag viscosity at steel surface; T_s: steel surface temperature; T_{sol}: slag solidification temperature; n: exponent for temperature dependence of viscosity, which is an empirical constant chosen to fit measured data.

Assuming the solid slag is attached to the mold wall, the boundary conditions for the liquid slag layer model, Eq.[1], are:

$$\text{solid/liquid slag layer interface: } V_z \Big|_{x=0} = V_s = V_m = \pi s f \cdot \cos\left(2\pi f t\right) \qquad [4]$$

$$\text{liquid slag/steel shell interface: } V_z \Big|_{x=d_l} = V_c \qquad [5]$$

where, V_s: solid slag layer velocity; V_m: mold velocity; V_c: casting speed; s: mold oscillation stroke; f: mold oscillation frequency.

Applying the boundary conditions Eqs.[4] and [5], Eq.[1] can be solved to obtain the following "pseudo-transient" analytical solution[25]:

$$V_z = \frac{-\left(\rho - \rho_{steel}\right)g x^{n+2}}{\mu_s \left(n+2\right) d_l^n} + \left(\frac{\left(V_c - V_s\right)}{d_l} + \frac{\left(\rho - \rho_{steel}\right)g d_l}{\mu_s \left(n+2\right)}\right)\frac{x^{n+1}}{d_l^n} + V_s \qquad [6]$$

where, d_l: liquid slag film thickness is calculated using the above heat transfer model.

To check the validity of the assumptions made to obtain Eq.[6], a fully transient numerical solution was obtained using an explicit finite-difference discretization with a central difference scheme and coded using MATLAB[26].

Figure 3 shows velocity profiles computed with these models based on heat transfer results for typical casting conditions given in Table I. For constant viscosity and a 0.2mm liquid layer, Fig. 3(a), shows the velocity profiles are linear. But when using the temperature dependent slag viscosity ($n=1.6$), the nonlinear effects are important. Figure 3 also compares the numerical solution and the pseudo-transient analytical solution. It shows that the transient effect is negligible for a film thickness of 0.2mm. Even for an extreme case, 2mm thick liquid film, the maximum transient effect is still less than 8%[25]. Therefore the pseudo-transient analytical solution to the liquid slag layer flow equation, Eq.[6] is a reasonable approximation of real transient solution.

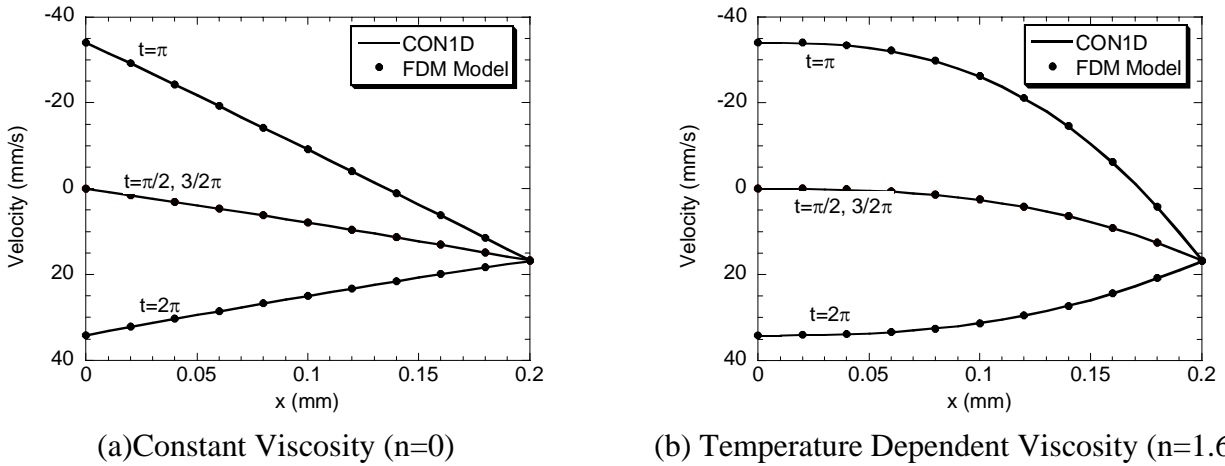(a) Constant Viscosity ($n=0$)   (b) Temperature Dependent Viscosity ($n=1.6$)

Fig. 3: Velocity profiles in liquid flux layer

Substituting Eq.[6] into Eq.[2] and evaluating at $x=0$ gives the shear stress at the interface between the liquid and solid slag layers:

$$\tau_{s/l} = \mu_s \frac{\left(n+1\right)\left(V_c - V_s(t)\right)}{d_l} + \frac{\left(n+1\right)}{\left(n+2\right)}\left(\rho - \rho_{steel}\right)g d_l \qquad [7]$$

4

Table I Casting Condition and Simulation Parameters (Case I with Slag A at 1.0m/min)

Carbon Content, $C\%$	0.05	%
Liquidus Temperature, T_{liq}	1529	^{o}C
Solidus Temperature, T_{sol}	1509	^{o}C
Steel Density, ρ_{steel}	7400	kg/m^2
Fraction Solid for Shell Thickness Location, f_s	0.3	-
Mold Powder Solidification Temperature, T_{fsol}	950	^{o}C
Mold Powder Conductivity, k_{solid}/k_{liquid}	1.5/1.5	W/mK
Mold Powder Viscosity at 1300°C, μ_{1300}	4.3	Poise
Exponent for Temperature dependence of Viscosity, n	1.6	-
Slag Density, ρ_{slag}	2500	kg/m^3
Mold Powder Consumption Rate, Q_{slag}	0.41	kg/m^2
Solid layer/mold interface friction coefficient, $\phi_{static}/\phi_{moving}$	0.4/0.4	-
Casting Speed, V_c	1.0	m/min
Pour Temperature, T_{pour}	1550	^{o}C
Slab Geometry, $W \times N$	1500$\times$230	mm$\times$mm
Working Mold Length, Z_{mold}	800	mm
Oscillation Mark Geometry, $d_{mark} \times w_{mark}$	0.45$\times$4.5	mm$\times$mm
Mold Oscillation Frequency, f	83.3	cpm
Oscillation Stroke, s	7.8	Mm
Time Step, dt	0.002	s
Mesh Size, dx	0.5	mm

Solid Slag Layer Stress Model

Near the meniscus, the solid slag layer attaches to the mold wall and oscillates with the mold. If the solid slag layer breaks and where it breaks could greatly affect heat transfer across the gap. A stress model is developed to investigate force balances and possible fracture in the solid slag layer.

Knowing that body forces F_z are negligible in the solid layer, the equilibrium force balance in the axial z-direction is:

$$\frac{\partial \tau_{xz}}{\partial x} + \frac{\partial \sigma_z}{\partial z} = 0 \qquad [8]$$

The maximum shear stress transmitted to the mold by friction with the solid slag layer due to relative motion of the mold and shell, τ_{max}, is:

$$\tau_{max} = \phi_{static} \cdot \sigma_x \qquad [9]$$

where, ϕ_{static}: maximum static friction coefficient between solid slag layer and mold wall; σ_x: normal stress, comes from the liquid steel ferrostatic pressure and the tiny head from the liquid slag pool above the meniscus.

Shear stress must be continuous across the gap, including both the boundaries at the mold and steel shell surfaces. When the liquid layer/steel side shear stress is smaller than the maximum solid contact shear stress,

then the friction force drops to match it. The shear stress on the mold wall is the minimum of the maximum static stress and the solid/liquid interface stress:

$$\tau_{mold} = Min\left(\tau_{s/l}, \tau_{max}\right) \qquad [10]$$

When shear stress in the liquid layer is greater than the maximum static friction stress, the solid layer tries to move along the mold. To maintain equilibrium without moving, axial stress builds up in the solid layer, which can be calculated based on Eq.[8].

To validate the solid slag layer stress model, a simplified case was solved using elastic finite-element stress analysis with ANSYS[27]. The boundary condition at the mold side had displacements fixed to zero and at the liquid side was ferrostatic pressure and shear stress (from CON1D). Table I gives the input conditions and simulation parameters used in CON1D. Figure 4 compares the stress results from ANSYS and CON1D. The CON1D model matches ANSYS except within 10mm near mold exit, where the real stress must quickly tend to zero (at atmospheric pressure). Detailed discussion of these results is given later.

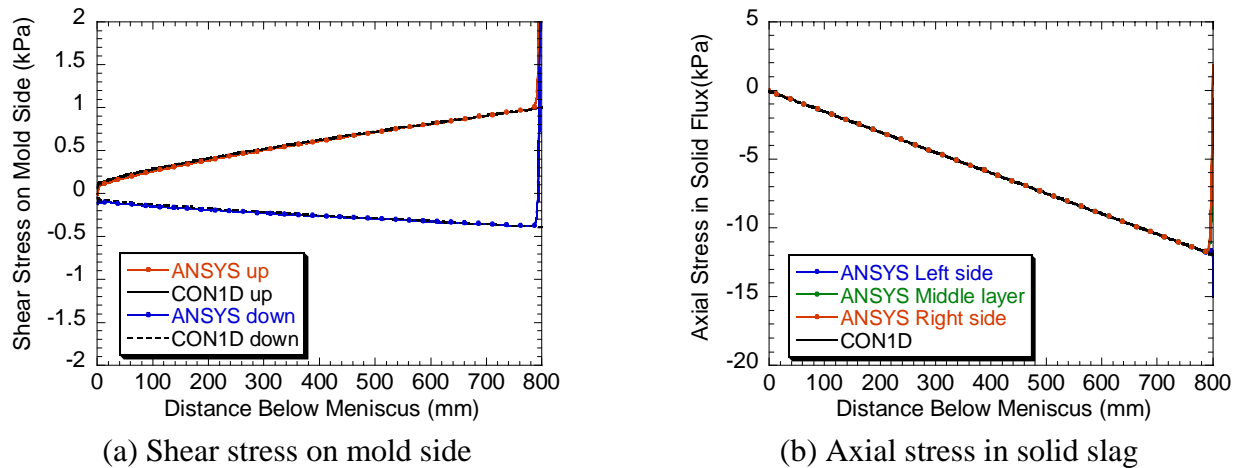(a) Shear stress on mold side   (b) Axial stress in solid slag

Fig. 4: Comparison of CON1D & ANSYS results: Shear Stress and Axial Stress in Solid Layer (Case I)

If the axial stress accumulated in solid slag layer exceeds the slag fracture strength, the solid slag layer will break, and be dragged down the mold wall. The shear stress on the mold/slag interface for this condition is:

$$\tau_{mold} = \phi_{moving} \cdot \sigma_x \qquad [11]$$

where, ϕ_{moving}: moving friction coefficient between solid slag layer and mold wall.

To satisfy the force balance: $\tau_{mold} = \tau_{s/l}$, substituting Eq.[11] into Eq.[7] can solve for the solid layer velocity when it slides from the mold wall. Fracture and sliding of the solid slag layer creates a gap between the upper attached solid layer and the lower moving layer. This gap will fill with liquid slag, and the solid layer might re-attach to the mold wall when the instantaneous velocity of the oscillating mold wall equals the moving solid slag layer velocity. The time for the liquid slag to fill the gap and the solid slag to re-attach depends on the slag consumption rate and liquid slag fluidity. The fracture and filling process causes extra slag consumption, which will decrease the liquid layer thickness and increase shear stress(/friction) for the whole mold.

Friction Model

The friction measured in operating casting molds may come from mold/slag contact, excessive taper, misalignment or a combination of the three.

6

Slag layer friction- Previous research has suggested that friction against the slag layer is important[28]. The liquid slag-layer flow model and solid slag-layer stress model described earlier give the shear stress on the mold wall, τ_{mold}, due to mold/slag contact. Integrating the shear stress along the mold face gives the total friction force due to contact between the mold and slag layers, $F_{contact}$:

$$F_{contact} = \int_0^{Z_{mold}} \tau_{mold} \cdot 2(W + N) \cdot dz \qquad [12]$$

where, Z_{mold}: working mold length; W: slab width; N: slab thickness

This model has been incorporated into CON1D, and will be used for the further detailed study described following.

Excessive taper- If the solid slag layer remains attached to the mold wall all the way down, there will be a thick liquid slag layer and low heat transfer across the mold/shell gap. Then the shell will have relatively high surface temperature and small shrinkage. In this case, excessive narrow face taper may squeeze the steel shell and therefore lead to increased friction. The maximum force from squeezing the shell occurs if the shell buckles, leading to longitudinal surface depressions, such as off-corner gutter in extreme cases[5], as shown in Fig. 5. Applying the Eular critical buckling load equation with rigid ends yields an estimate of the normal stress on the mold wall:

$$F_{cr} = \frac{4\pi^2 EI}{L_{eff}^2} = \frac{4\pi^2 E}{L_{eff}^2} \frac{b^3 h}{12} \qquad [13]$$

Where, b: shell thickness; h: vertical contact length along the narrow face; L_{eff}: unsupported shell width along wide face from the corner; E: steel elastic modulus.

So the friction due to buckling for each narrow face is:

$$F_{excessive\ taper} = 2\phi_{static} \cdot F_{cr} \qquad [14]$$

Misalignment friction- Misalignment of the mold and strand is another important potential cause of friction. The friction force during each oscillation cycle is the difference between the force transducer measurements with and without steel casting[29]. Currently, such friction signals are used to detect misalignment problems in real casters.
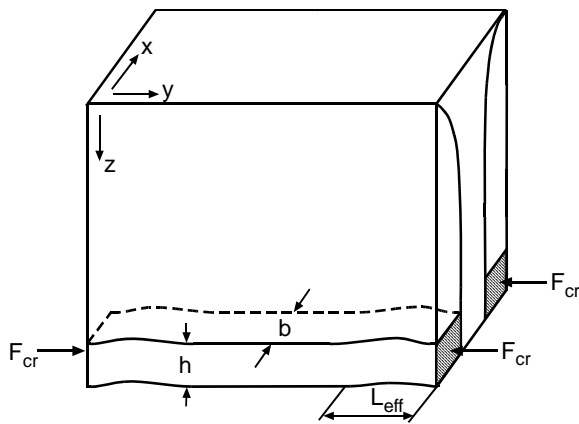

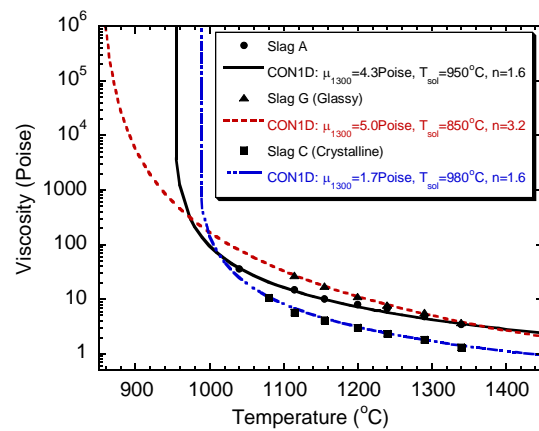Fig. 5: Schematic of friction forces from excessive taper of narrow mold faces

Fig. 6: Mold slag viscosities modeled in this work

EXAMPLE APPLICATION

The CON1D model is used to simulate behavior of typical casting conditions listed in Table I. During casting mold slag may absorb reoxidation products such as alumina. This changes the slag composition and its properties. Alumina tends to decrease slag basicity, which decreases the crystallization temperature and increases viscosity at high temperature[22, 30]. This makes the slag easier to be glassy. Figure 6 shows the viscosity curves vs. temperature, which were chosen to match with the measured slag viscosity data reported by Lanyi[22]. The typical continuous casting Slag A might be crystalline or glassy (Slag A2 in Lanyi); Slag C is easier to be crystalline (Slag A6 in Lanyi). Slag G is Slag C with 25% additional alumina, which has high tendency to be glassy[22]. The composition and properties of these three slags are listed in Table II.

Table II   Slag Composition and Properties

Slag	CaO	SiO$_2$	Al$_2$O$_3$	MgO	Na$_2$O	K$_2$O	F$_2$	FeO	MnO	B$_2$O$_3$	T_{fsol}	n	μ_{1300}
	wt%	wt%	wt%	wt%	wt%	wt%	wt%	wt%	wt%	wt%	°C	-	P
A	32.3	36.4	8.9	0.7	5.0	1.9	8.3	3.0	-	3.4	950	1.6	4.3
G	27.5	30.3	21.4	0.9	5.6	-	12.0	1.1	1.3	-	850	3.2	5.0
C	34.8	38.3	0. 5	1.2	7.1	-	15.2	1.4	1.6	-	980	1.6	1.7

Table III   Case Study Parameters

	Case I	Case II	Case III
Lubrication Consumption, $Q_{lub:}$	0.2kg/m^2	critical	0.2kg/m^2
Solid Layer Status:	attached	attached	moving

Table IV   Mold Oscillation Practice with Casting Speed

Casting Speed, V_c	Oscillation frequency, f	Negative Strip Time, NST	Negative Strip ratio, $NS\%$	Osc. Mark, $d_{mark} \times w_{mark}$	Osc. Marks Consumption, Q_{oscg}
m/min	cpm	s	-	mm×mm	kg/m^2
1.0	83.3	0.24	0.3	.45*4.5	0.21
1.3	108.3	0.19	0.3	.30*3.0	0.094
1.6	133.3	0.15	0.3	.16*1.6	0.027
2.0	166.7	0.12	0.3	0*0	0
3.0	250.0	0.08	0.3	0*0	0
5.0	416.7	0.05	0.3	0*0	0

Computation of both heat transfer and friction depends greatly on the total consumption rate of slag into the gap, Q_{slag}(kg/m^2), which is an input parameter in this work. It is important to introduce the concept of "lubricating consumption rate": Q_{lub}, which is the slag consumption not carried inside the oscillation marks:

$$Q_{lub} = Q_{slag} - Q_{osc} \qquad [15]$$

where, Q_{osc}: the consumption rate of slag carried within the filled oscillation marks is found from:

$$Q_{osc} = 0.5\rho \cdot d_{mark} \cdot w_{mark} / L_{pitch} \qquad [16]$$

where, d_{mark}: oscillation marks depth; w_{mark}: oscillation marks width; L_{pitch}: oscillation pitch length.

The liquid slag represented by Q_{lub} acts to lubricate the mold-shell interface and thereby lower friction. The CON1D model is run with different mold slags, consumption rates and casting speeds to study the effect of mold powder properties and oscillation practice. The related parameters are listed in Tables II to IV.

(a) Heat Flux

(b) Shell and Mold Temperature

(c) Steel Shell Thickness
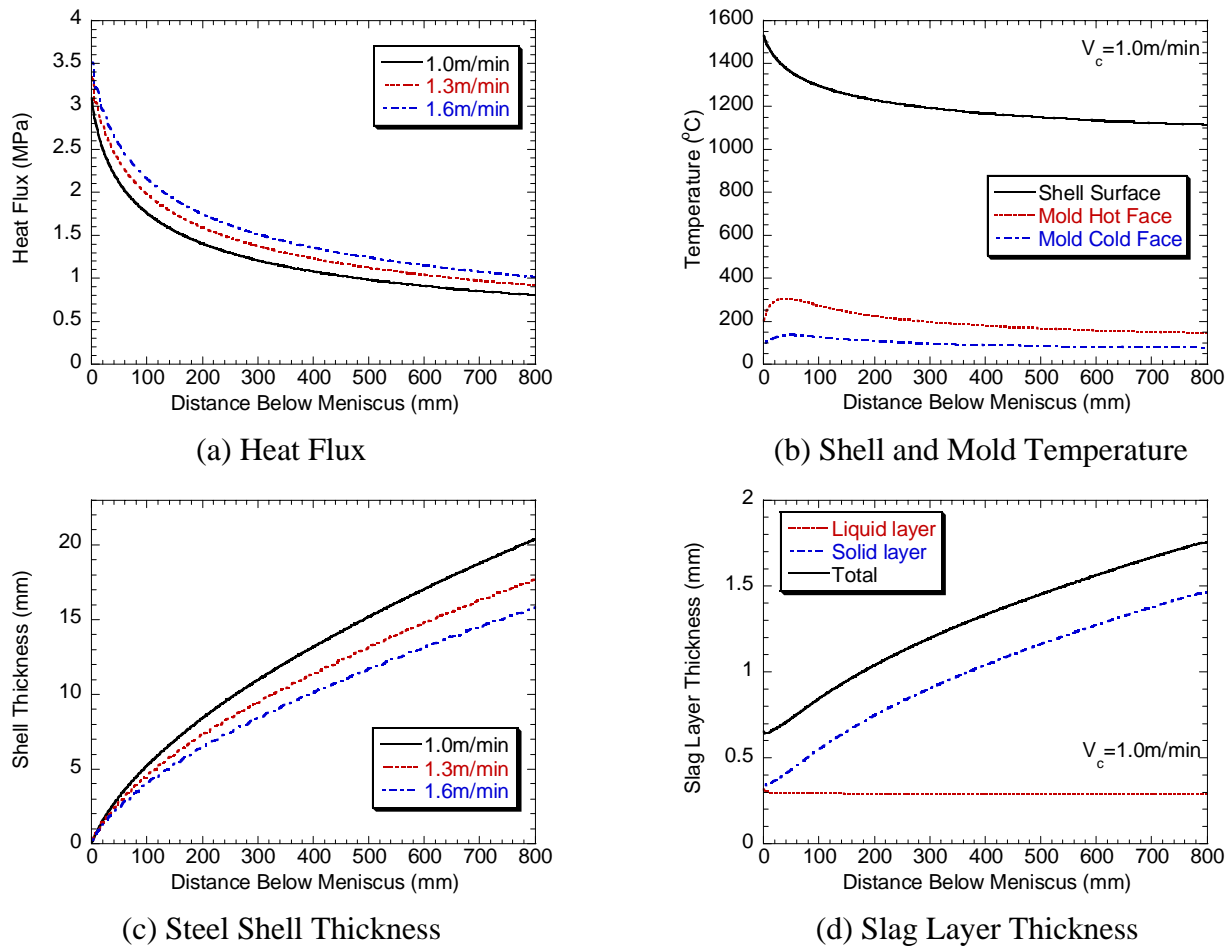
(d) Slag Layer Thickness

Fig. 7: Typical results of Case I with Slag A

Typical Results

Simulations were first run for typical low friction conditions, assuming that all solid slag is attached to the mold wall. Case I series run with a stable lubrication consumption rate Q_{lub}, 0.2kg/m^2, first at 1.0m/min casting speed (total consumption rate, Q_{slag}=0.41kg/m^2). Figure 7 shows some typical results of run with Slag A. The mean heat flux in the mold is 1.24MW/m^2 and the shell thickness is 20.4mm at mold exit assuming solid fraction is 0.3. A uniform liquid slag layer, 0.29mm is shown in Fig. 7(d), while the solid layer continually increases. The thick solid layer was assumed to built up over time starting during initial mold filling with starter slag. Once it reaches steady state, it does not consume any new mold powder.

Figure 8 shows the cooling history of various points in the slag layer for Case I with Slags A and G. The TTT curve of a conventional industrial mold slag (7.9% Al$_2$O$_3$)[31] is used to estimate the onset of crystallization for Slag A. Fig. 8(a) predicts crystallization in most of slag layer except the very thin layer (0.2mm) adjacent to the mold wall. Extra alumina in the slag delays the onset of crystallization and increases the temperature range of crystallization, so the TTT curve of slag with 19.5% Al$_2$O$_3$[32] is used to estimate the onset of crystallization for Slag G. Fig. 8(b) shows that no points in Slag G crosses the TTT curve, so no crystalline phase is predicted. This agrees with the assumption that Slag G tends to be glassy.

Shear stress and axial stress along the solid slag layer was plotted in Fig. 4. It shows that the solid slag layer is in compression almost everywhere. So the attached solid slag layer is stable and no fracture will occur. This can happen in practice, as evidenced in the recovery of a solid slag layer attached to the mold wall after one hour of casting, which contains trace elements only found in the starter slag (consumed in the first few minutes)[33]. The stable, thick liquid layer ensures a very low friction force on the mold wall.
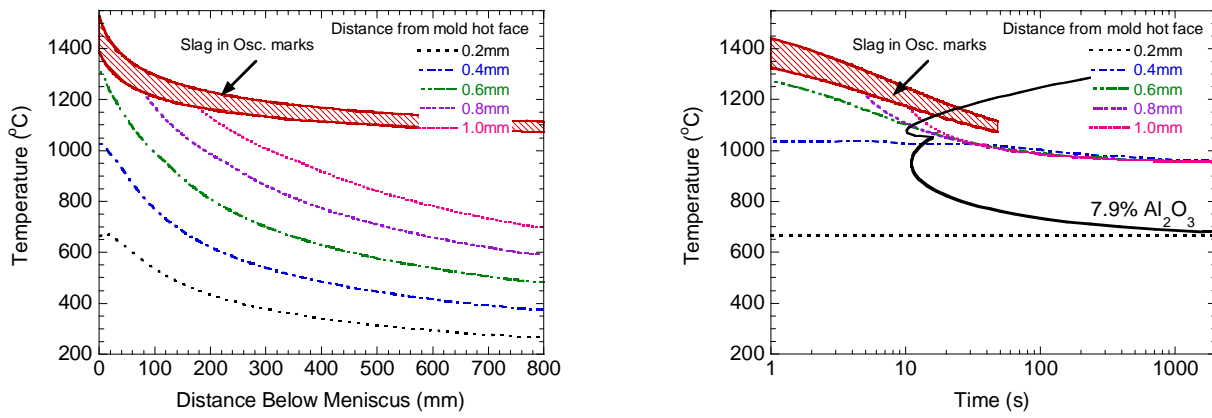
(a) Slag A (Crystalline)
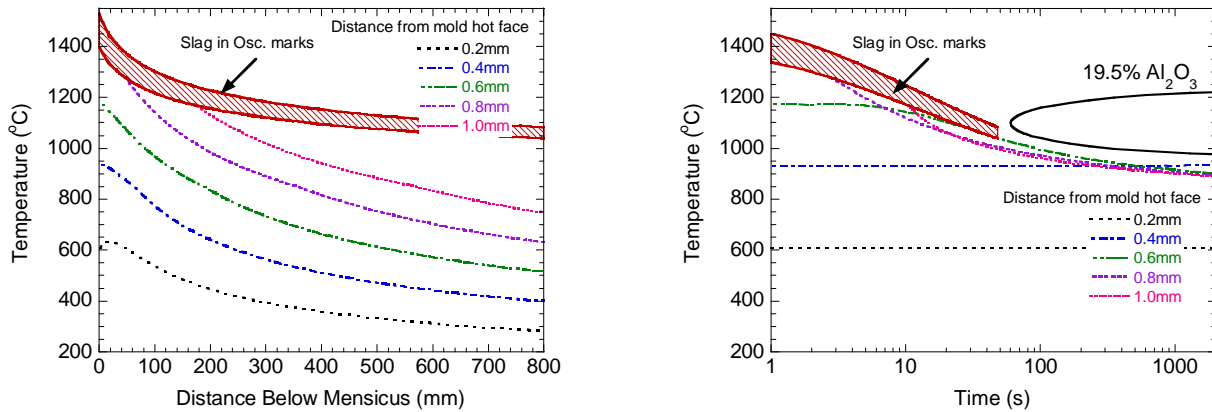
(b) Slag G (Glassy)

Fig. 8: Slag layer cooling history with TTT curves[31, 32]

Critical Slag Consumption Rate

Lower slag consumption rate, Q_{lub}, leads to higher shear stress in the liquid/solid slag interface. If friction on the mold side cannot balance the shear stress along the solid/liquid interface, axial tensile stress must build up in solid slag layer to compensate. When axial stress in the solid slag exceeds the slag fracture strength, the solid slag breaks and is dragged down the mold wall. The critical consumption rate is the minimum consumption rate to keep solid slag attached to the mold wall without breaking or sliding. In order to find it, the complete model CON1D is run several times with different consumption rates, Case II, assuming slag fracture strength of 80MPa[34]. Figure 9 shows the axial stress and shear stress distribution of two slags along the mold wall at the critical consumption rate. It shows that tensile axial stress accumulates in the solid slag only when liquid shear stress exceeds maximum static solid friction. In each case, fracture is predicted during upstroke when axial stress is greater than slag fracture strength. All stresses are compressive during the down stroke.

Slag G has 60% larger critical lubricating consumption rate, Q_{lub}, 0.12kg/m^2 than Slag A, 0.075kg/m^2.Slag C has similar behavior to Slag A, but with an even lower critical Q_{lub}, 0.05kg/m^2. The most important difference between Slag A/C and G is the position of slag fracture. For crystalline slags A, C, the solid slag layer fractures within 100mm near meniscus while the glassy slag G fractures near mold exit. These results show that the sharpness of the slag viscosity increase near solidification temperature is more important than the popular slag property, slag viscosity at 1300°C.

Figure 10 compares the heat flux and mold temperature of these two critical cases. Very high heat flux is predicted near the meniscus, especially for slag A. This is also indicated by the high mold temperature at that region. It implies that in a real caster, if an abnormal high mold temperature is observed near the meniscus, it

may due to a temporary consumption rate drop, which should also correlate with the solid slag breaking and moving down the mold wall. Slag fracture in turn will cause temporary gaps, heat flux drops, and thermal stresses in the shell. This phenomenon of high meniscus heat flux and high variations is known to correlate with strand defects, which is consistent with the model prediction here.
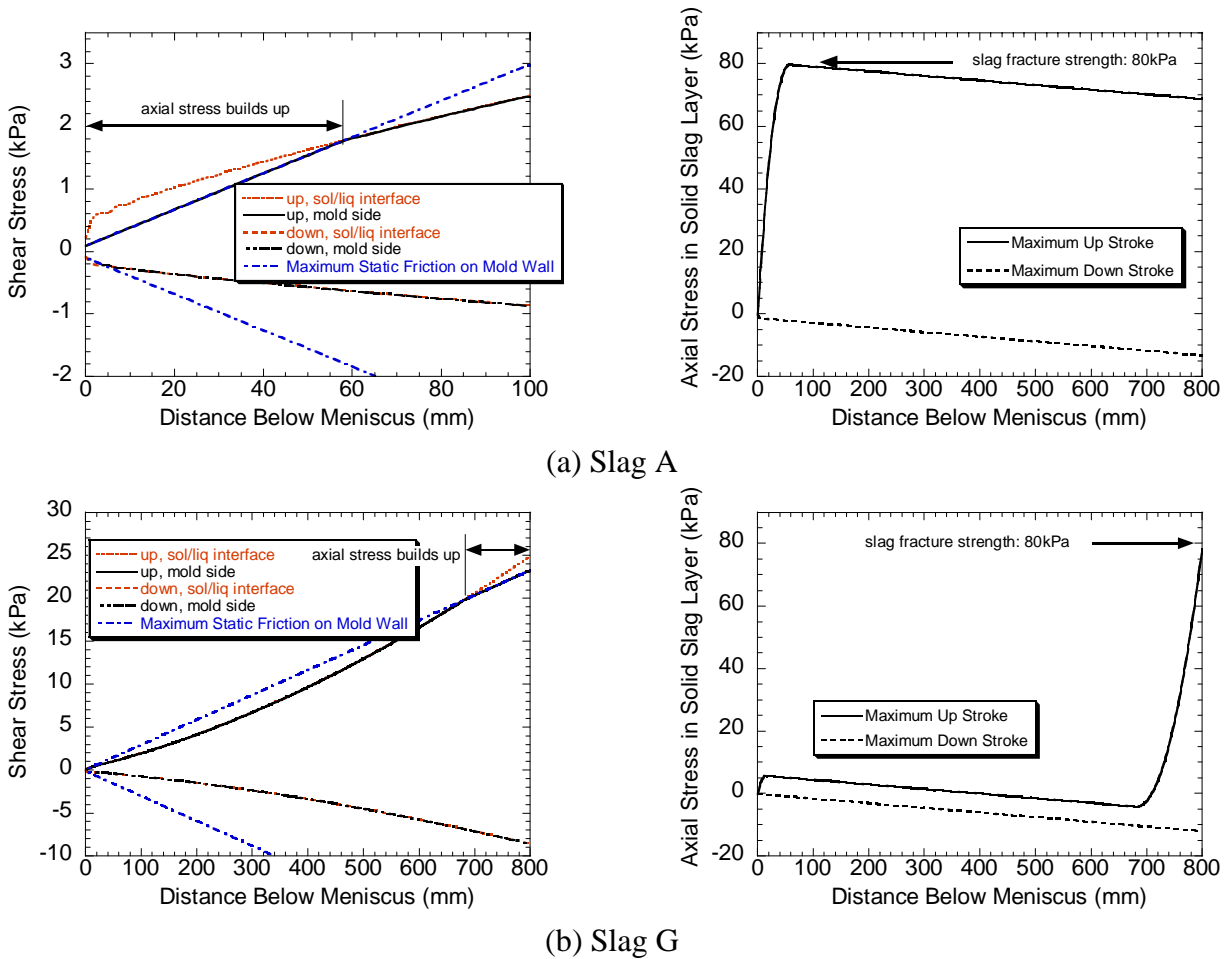

(a) Slag A

(b) Slag G

Fig. 9: Effect of Slag type on axial stress build up in solid layer for critical Q_{lub}
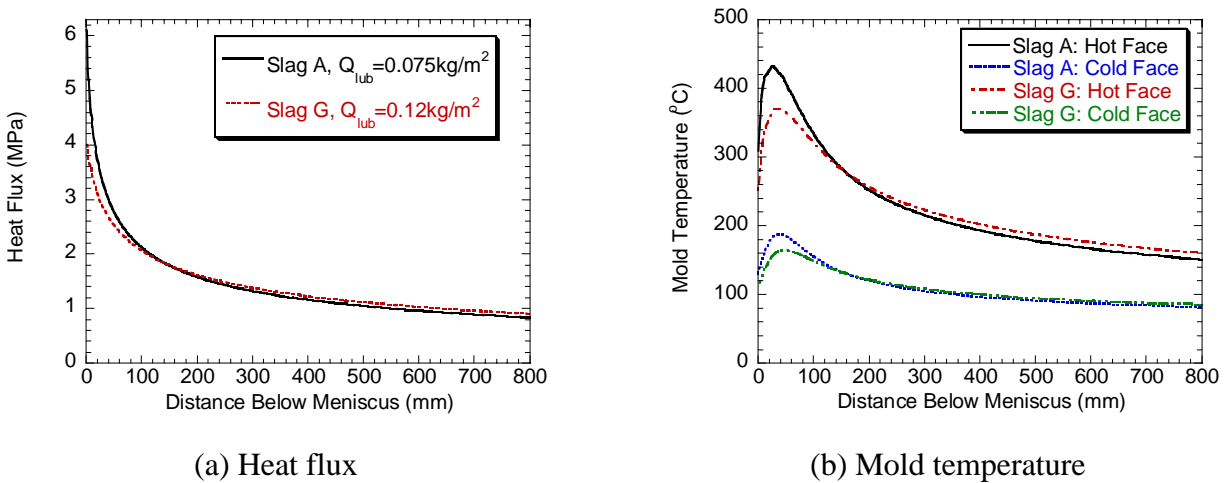

(a) Heat flux

(b) Mold temperature

Fig. 10: Comparison of heat flux and mold temperature with critical consumption rate

Mold Friction

Attached slag layer- When casting with a stable conventional consumption rate (Q_{slag}=0.41kg/m^2), the model predicts a stable solid slag layer and a very low friction force. For the cases studied here, the mold wall shear stress amplitude is 0.85MPa for slag A, and 2.52MPa for slag G, which are far lower than reported measured friction data[35]. The high friction force measured in operating casters likely comes from three possible causes: a moving solid slag layer, excessive taper or misalignment.

Moving solid slag layer- If the liquid slag level at the meniscus varies, it cannot keep a steady flow into the mold/strand gap even assuming the mold taper and alignment are reasonable and do not contribute to friction. The solid slag layer may break and move along the mold wall, accounting for part of the slag consumption. For a given consumption rate, the liquid slag layer is thinner when the solid layer moves. This leads to higher heat flux and higher friction and therefore perpetuates the slag fracture and motion. The fracture position predicted for slag A (Case II with critical consumption rate), is near the meniscus, thus, the low viscosity liquid layer may quickly fill in the gap due to facture, and the solid slag layer can reattach to the mold wall until the next fracture. For slag G, if the consumption temporarily drops lower than the critical consumption rate, the solid slag layer fracture will occur further above mold exit. Reattachment is more difficult. For simplification, the solid slag layer velocity is assumed to average some small constant percentage of the casting speed, v_f. In case III, assuming $v_f \approx 5\%$ produces total friction force prediction within the measured range of 15~23kPa[35]. Note the average "moving" solid slag layer velocity is not the physical moving speed of solid layer. It is only used to calculate powder consumption due to the intermittent procedure of the solid layer fracture, moving and re-attaching. Most of time the solid layer still sticks to the mold wall, so the shear stress can still be calculated based on liquid layer friction and maximum static friction between mold and solid layer. Figure 11 shows that both liquid layer and solid layer with "moving" layer are thinner than the attached case. Especially the liquid slag layer gets thinner with the distance down the mold and nearly runs out at mold exit. This increases friction greatly.

Fig. 11: Slag layer thickness with "moving" solid layer (Slag A)

(a) Casting speed and mold velocity

(b) Attached solid layer (Case I)

(c) "Moving" solid layer (Case III)

Fig. 12: Velocity and shear stress during half oscillation cycle

Friction variation during an oscillation cycle- Figure 12(a) shows the mold velocity and casting speed profile during half of one oscillation cycle. It shows that at 0.24second, the mold velocity is equal to the casting speed, which means that the mold moves down with the steel shell, so there is no shear stress at that instant.
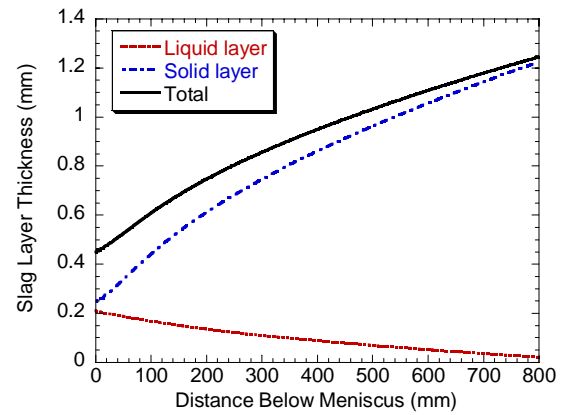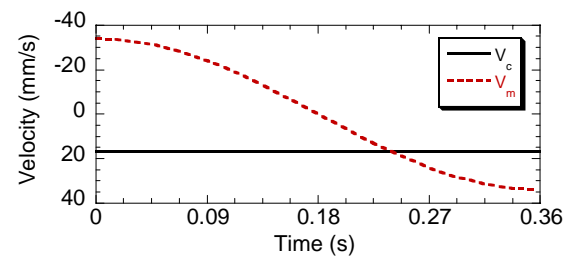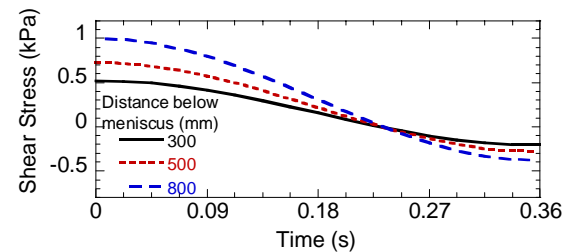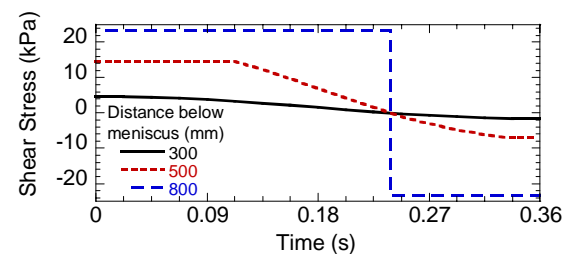
12

After that time, the mold moves down faster than shell during the period of "negative strip". Thus, the stress acting on slag layer shifts from tension to compression. Figure 12 also shows that the shear stress on the mold wall with a "moving" solid slag layer, (c), is much higher than with an attached layer, (b). Shear stress increases with distance along the mold length, and the transition from tension to compression becomes sharper for a moving layer.

In the upper mold, liquid slag controls the friction between mold and shell, so the shear stress is nearly sinusoidal. In the lower mold region, the solid slag layer controls friction and the shear stress profile tends toward a square wave. Figure 13 shows the shear stress down the mold at different times during the oscillation cycle. For all lines, there is a transition from curved to straight, where liquid slag layer control transfers to solid slag layer control. The "average" is the mean of the absolute values of all the shear stresses over the whole oscillation cycle, and is very near to the curve when V_m is zero. This means that the average friction force can be estimated with a simple static mold model. Integrating the shear stress over each mold face at each instant gives the total friction force history shown in Fig. 14 for different cases.

Total mold friction- Figure 14 shows that the friction due to shear stress is very small if the solid slag layer is attached and there are no other sources of friction. Another possible cause of high friction may be squeezing of the steel shell due to excessive narrow face taper. This is most likely when the shell temperature is high and shrinkage is small at high casting speed. A rough estimation of the magnitude of this friction is 15kN on each narrow face, based on Eqs.[13], [14], assuming buckling happens over the last 10mm (h=10mm) near mold exit, shell thickness b=20mm, L_{eff}=600mm, E=25GPa at 1100°C. This corresponds to an average friction stress over a 800mm long 230mm thick and 1500mm wide slab mold of 10kPa, which is similar to measured data[35]. Figure 14 shows the friction force during oscillation cycle. Excessive taper can be identified by its shape of the friction force curve being almost square. In contrast, liquid slag lubrication produces a smooth curve. Thus the lubrication/friction state of the mold can be identified from the shape of the friction force curve during an oscillation cycle in addition to its magnitude. And misalignment curves should be curved (not square) according to the gap thickness changes during the cycle.
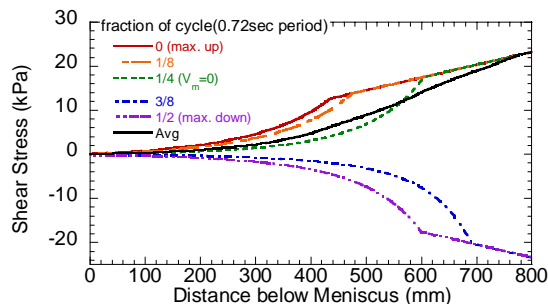

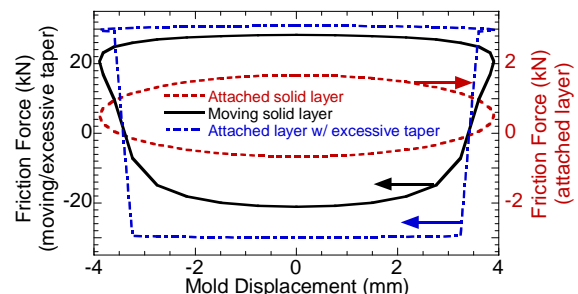Fig. 13: Shear stress down the mold wall with "moving" solid layer (Slag A)

Fig. 14: Total friction force during an oscillation cycle (Slag A)

CONSUMPTION AND CASTING SPEED STUDY

Effect of Slag Properties on Critical Consumption Rate

The most important parameter affecting slag shear stress and fracture is the liquid slag consumption rate. So long as consumption rate exceeds a minimum critical rate, the slag will not fracture. A parametric study was conducted on the minimum critical consumption to keep a stable attached solid slag layer. First, the effects of slag Poisson's ratio, liquid slag pool depth, mold thickness on critical consumption rate are found negligible. A strong mold slag (doubling fracture strength) allows the critical Q_{lub} for slag A to decrease only by 7% and delay the fracture from 60mm to 100mm below meniscus. The fracture strength has even less effect for slag G.

Maintaining high mold/slag friction coefficient is important to lower the critical consumption. As shown in Fig.15, especially for slag G, when friction coefficient is lower than 0.15, the slag layer can fracture, even for stable conventional consumption rate.

Oscillation marks act as an extra resistance layer between the liquid slag layer and the steel shell. Thus they slightly lower temperature in liquid layer, which leads to higher viscosity liquid, higher shear stress, easier flux fracture and higher critical consumption. Specifically, 0.45mm*4.5mm oscillation marks cast at 1.0m/min increase Q_{lub} by 0.01kg/m^2 for both slags (15% for slag A and 9% for slag G) relative to cases with no oscillation marks.

Effect of Casting Speed on Critical Consumption Rate

The influence of casting speed on mold friction and interface heat flux has been investigated in a parametric study. Based on Case I, the casting speed varied from 1.0m/min to 5.0m/min. The stroke was fixed at 7.8mm, and oscillation frequency adjusted to keep a constant negative

Fig. 15: Effect of friction coefficient on critical consumption rate

strip ratio of 0.3 and a constant pitch length of 12mm. Negative strip time thereby decreases with increasing casting speed, so oscillation mark depth decreases. The powder consumption rate thus decreases due to the shallower oscillation marks and higher oscillation frequency. Oscillation marks are assumed negligible when casting speed is greater than 2m/min. Table IV gives the mold oscillation parameters used. Those parameters are chosen based on some previous plant measurements of oscillation marks depth[36] and total mold powder consumption rate[8, 37-39] as shown in Figs. 16 and 17.
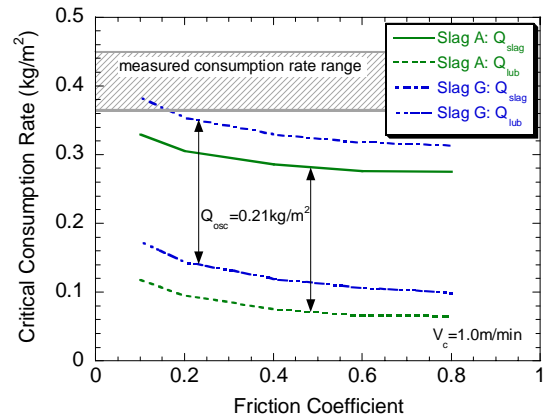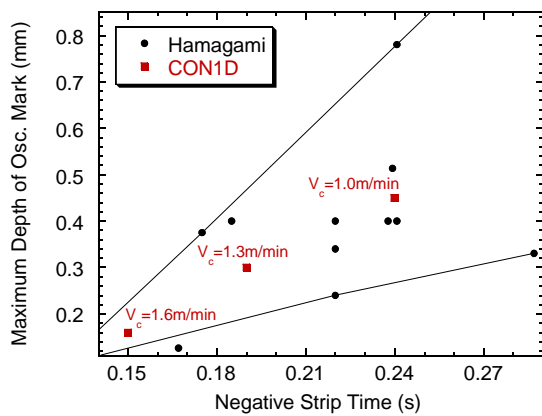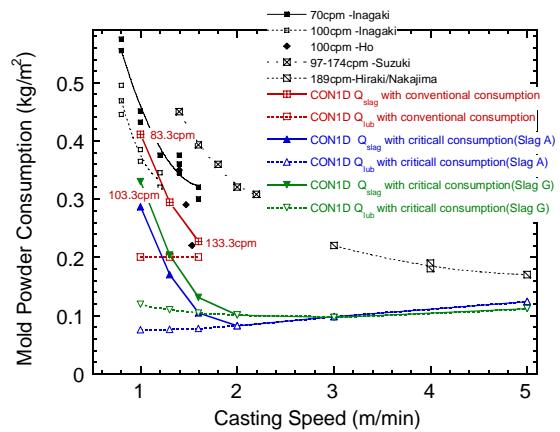

Fig. 16: Maximum oscillation marks depth

Fig. 17: Powder consumption rates

Figure 17 also compares measured consumption rates[8, 37-39] with critical consumption rates calculated in this study. Measured consumption rates exceed the critical rates, which indicates that slag fracture should be a rare transient event. If the total consumption rate can be steadily maintained, the strand should be well lubricated and a stable solid slag layer should remain attached to the mold. Figure 17 shows that measured consumption rates decrease with increasing casting speed. When there is significant consumption by the oscillation marks, Q_{osc}, the critical consumption also decreases with increasing casting speed. This is because oscillation mark depth decreases, carries less slag and increases the lubrication consumption component to help solid layer attached to the mold wall as explained above. However, at higher casting speed (>2m/min), when the oscillation mark effect is negligible, the critical consumption rate increases slightly with casting speed.

14

Figure 18 shows two opposing effects of different casting speed on solid slag fracture, excluding oscillation marks and their effects. Increasing casting speed increases the velocity difference between mold and shell, which tends to increase friction. It also increases shell surface temperature, which tends to decrease slag viscosity and friction. For slag A, the first effect prevails, so the slag always fails near meniscus and higher casting speed is more dangerous to slag fracture. To be specific, increasing V_c from 1.0m/min to 2.0 m/min, requires the critical Q_{lub} to increase by 25%. Also, the fracture position occurs closer to the meniscus (moving from 60mm to 30mm). When the critical fracture position is near to the mold exit, such as slag G, the effect of higher surface temperature predominates, so higher casting speed helps to avoid slag fracture, as shown in Fig. 18(b). Thus, increasing casting speed from 1.0m/min to 2.0m/min decreases critical Q_{lub} by 8%. However, further increasing casting speed above 3.0m/min causes the critical fracture position to move to near the meniscus, and increases the critical Q_{lub} as for slag A.

	V_c (m/min)	Q_{lub} (kg/m²)
——	1.0	0.066
—·—·	1.3	0.071
– – –	1.6	0.076
- - -	2.0	0.082
—··—··	3.0	0.098
------	5.0	0.124

(a) Slag A

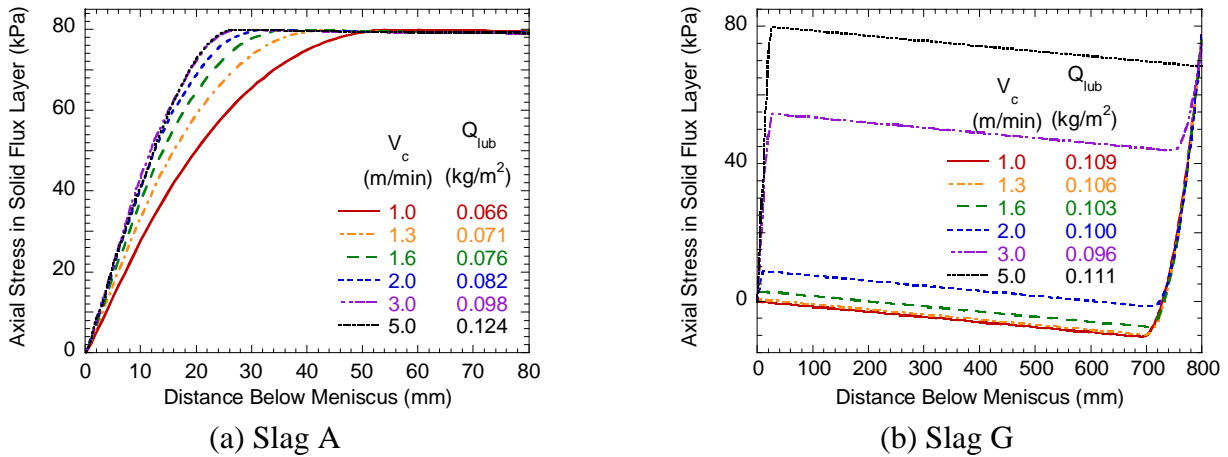|	V_c (m/min)	Q_{lub} (kg/m²)
——	1.0	0.109
—·—·	1.3	0.106
– – –	1.6	0.103
- - -	2.0	0.100
—··—··	3.0	0.096
------	5.0	0.111

(b) Slag G

Fig. 18: Effect of casting speed on solid slag fracture (no oscillation marks)

Note that the minimum critical consumption rate occurs at intermediate speed (~2m/min) for the conditions of this study, which is the safest speed for slag layer stability. Measured consumption rates exceed the calculated critical consumption rates by the largest factor (~3X) for this intermediate speed. Safety margins are less at both lower speed and higher speed. At very high speed, ~5m/min, measured consumptions approach critical levels, indicating that solid slag layer stability becomes a general problem at high speed.

Also, average mold heat flux increases with higher casting speed, with lower consumption rate or with a moving solid slag layer, refer to Figs. 7 and 10. High and variable heat flux is another indication of slag layer fracture.

Effect of Casting Speed on Friction Stress

Finally, CON1D was run with a detached solid slag layer moving at an average velocity of 6% of the casting speed and 4% for slag G (Case III). The lubrication consumption rate Q_{lub} was assumed to remain the same, 0.2kg/m^2, for all cases. The solid friction force with moving slag is much higher than for attached cases, and decreases with increasing casting speed. These predictions compare with measured data[35], as shown in Fig. 19. The agreement at lower casting speed (1.0m/min) confirms the prediction that solid slag fracture and movement increases at lower speed. The high friction at high speed is likely due to other friction sources such as excessive mold taper. It is interesting that the drop in friction at intermediate speed roughly corresponds to the minimum in critical consumption rate and maximum safety factor.

Fig. 19: Effect of casting speed on friction force: measurement and prediction

CONCLUSIONS

Analytical transient models of liquid slag flow and solid slag stress are coupled with a finite-difference model of heat transfer in the shell and mold. All three models have been validated extensively with plants measurements. They are applied to study the effect of casting speed and mold powder properties on slag layer behavior between the oscillating mold wall and solidifying steel shell. Specific conclusions are:

1. Solid slag generally remains attached to the mold wall, especially near the meniscus. When friction on the mold side cannot compensate the shear stress on the slag solid/liquid interface, axial stress builds up in the solid slag layer. If powder consumption rate drops below a critical level, the axial stress can exceed the slag fracture strength, so the solid slag breaks and moves down the mold wall.

2. The slag temperature-viscosity curve determines the shear stress along the mold wall and affects both the critical consumption rate and possible fracture position. Crystalline slag A (with a sharp viscosity transition) tends to fracture near the meniscus, but less easily (lower critical Q_{lub}). Glassy slag G (with gradual rise at lower temperature) tends to fracture near mold exit easily (higher critical Q_{lub}). Increasing melting temperature and decreasing high-temperature viscosity (such as occurs with high basicity slag) tends to lower critical Q_{lub} and make it less easy to fracture.

3. A parametric study reveals the variables which increase axial stress in the solid slag layer, critical Q_{lub}, and the likelihood of slag fracture.
   - Increasing friction coefficient helps the solid slag stay attached to the mold wall.
   - Oscillation marks increase the danger of slag fracture due to the extra thermal resistance leading to lower temperature, higher liquid slag viscosity and higher gap friction.
   - When slag fracture occurs near the meniscus, such as for slag A and for slag G cast>3.0m/min, increasing casting speed increases the danger of slag fracture, and requires higher critical Q_{lub}.
   - When slag fractures near mold exit, such as slag B cast<3m/min, increasing casting speed is safer for avoiding slag fracture.
   - Increasing slag fracture strength provides little help for glassy slags (slag G). Doubling fracture strength of crystalline slag A allows Q_{lub} to decrease by 7% and delays the fracture position from 60mm to 100mm below meniscus.

4. Liquid slag layer lubrication can be recognized by very low mold shear stress with a sinusoidal variation over each oscillation cycle. Solid slag layer fracture and movement generate high friction with a square wave.
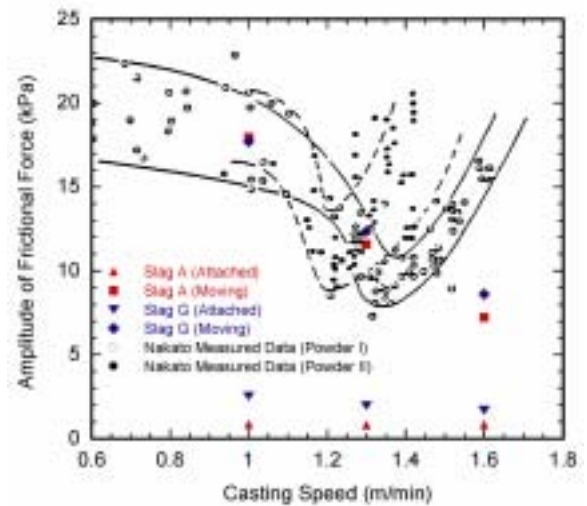
16

5. The top half of the mold has lower friction, as a liquid slag layer controls friction. Solid slag friction begins when liquid slag nearly runs out towards the bottom of the mold. The fraction of the mold with solid slag friction can be identified by:
   - magnitude of measured mold friction (more solid slag tends toward higher friction)
   - shape of friction over each cycle (more solid slag tends toward sharper "square" transition)
6. For a stable attached solid slag layer during casting, the mold friction is very small (~1kPa scale). The roughly 10X higher friction measured in real casters might be due to any of three sources: an intermittent moving slag layer, excessive taper or mold misalignment. At low casting speed, the critical consumption rate is high, so variations in consumption at the meniscus can easily lead to solid slag layer fracture and movement. At high casting speed, excessive taper and mold misalignment likely increase friction problems.

ACKNOWLEDGMENTS

REFERENCES

1. M.M. Wolf, "Mold heat transfer and lubrication control two major functions of caster productivity and quality assurance," in Continuous Casting 1997, Vol. Volume 9: Initial Solidification and Strand Surface Quality of Peritectic Steels, Iron and Steel Society/AIME, 1997, pp. 211-22.

2. K.C. Mills, S. Sridhar, A.S. Normanton, S.T. Mallaband, "Mould flux behaviour in continuous casting," The Brimacombe Memorial Symposium, (Vancouver, British Columbia, Canada), 2000, pp. 781-794.

3. T.J.H. Billany, A.S. Normanton, K.C. Mills, P. Grieveson, "Surface Cracking in Continuously Cast Producs," Ironing and Steelmaking, Vol. 18 (6), 1991, pp. 403-410.

4. R. Bommaraju, R. Glennon and M. Frazee, "Analysis of the Cause and Prevention of Longitudinal Midface Cracks and Depressions on Continuously Cast Free-Machining Steel Blooms," 1st European Conference on Continuous Casting, (Florence, Italy), Vol. 1, 1991, pp. 1.599-1.610.

5. B.G. Thomas, A. Moitra and R. McDavid, "Simulation of longitudinal off-corner depressions in continuously cast steel slabs," Iron and Steelmaker (USA), Vol. 23 (4), 1996, pp. 57-70.

6. E. Takeuchi and J.K. Brimacombe, "The Formation of Oscillation Marks in the Continuous Casting of Steel Slabs," Metall. Trans. B, Vol. 15B (3), 1984, pp. 493-509.

7. C.A. Pinheiro, I.V. Samarasekera and J.K. Brimacombe, "Mold Flux for Continuous Casting of Steel," I&SM, Vol. 22 (9), 1995, pp. 37-39.

8. M. Suzuki, H. Mizukami, T. Kitagawa, K. Kawakami, S. Uchida, Y. Komatsu, "Development of a new mold oscillation mode for high-speed continuous casting of steel slabs," ISIJ International (Japan), Vol. 31 (3), 1991, pp. 254-261.

9. M.M. Wolf, "Review of Mould Fricrtion," BHM, Vol. 145 (7), 2000, pp. 270-275.

10. M.R. Ozgu and B. Kocatulum, "Thermal Analysis of the Burns Harbor No. 2 Slab Caster Mold," 76th Steelmaking Conference, (Dallas, Texas, USA), Vol. 76, 1993, pp. 301-308.

11. G.A. Geist, "Establishing mold thermal stability and lubrication during continuous casting of high carbon steel grades," 83rd Steelmaking Conference, (Pittsburgh, PA, USA), Vol. 83, 2000, pp. 389-396.

12. C. Orrling, A.W. Cramb, A. Tilliander, Y. Kashiwaya, "Observations of the melting and solidification behavior of mold slags," Iron and Steelmaker (USA), Vol. 27 (1), 2000, pp. 53-63.

13. D.T. Stone and B.G. Thomas, "Measurement and modeling of heat transfer across interfacial mold flux layers," <u>Canadian Metallurgical Quarterly (Netherlands),</u> Vol. 38 (5), 1999, pp. 363-375.

14. R.J. O'Malley, "Observations of various steady state and dynamic thermal behaviors in a continuous casting mold," 82nd Steelmaking Conference, (Chicago, IL, USA), Vol. 82, 1999, pp. 13-33.

15. Y. Meng and B.G. Thomas, "Heat Transfer and Solidification Model of Continuous Slab Casting: CON1D," <u>Metall. Mater. Trans. B (USA)</u> (submitted), 2002.

16. T. Cimarelli, "Mould powder influence on continuous casting operations and on slabs surface quality," <u>Metallurgia Italiana (Italy),</u> Vol. 89 (9), 1997, pp. 31-37.

17. G.J.W. Kor, "An Analysis of the Fluid Flow of Liquid Mold Powder in the Space Between the CC Mold and the Steel Shell," Continuous Casting of Steel, 2nd Process Technology Conf., (Chicago, Ill., USA), Vol. 2, 1981, pp. 124-132.

18. I.B. Risteski, "A Mathematical Model of the Movement of Molten Powder in the Vicinity of the Meniscus During the Continuous Casting of Steel," <u>Revista de Metalurgia (Spain),</u> Vol. 28 (5), 1992, pp. 288-296.

19. J.M. Hill and Y.H. Wu, "On a Nonlinear Stefan Problem Arising in the Continuous Casting of Steel," <u>Acta mech.,</u> Vol. 107 (1-4), 1994, pp. 183-198.

20. J.A. DiLellio and G.W. Young, "Asymptotic model of the mold region in a continuous steel caster," <u>Metallurgical and Materials Transactions B: Process Metallurgy and Materials Processing Science,</u> Vol. 26B (6), 1995, pp. 1225-1441.

21. J.F. Chavez, A. Celaya, M.A. Barron, R.D. Morales, "Heat transfer in mold flux-layers during slab continuous casting," Seventy Ninth Conference of the Steelmaking Division of the Iron and Steel Society, (Pittsburgh, Pennsylvania, USA), Vol. 79, 1996, pp. 321-329.

22. M.D. Lanyi and C.J. Rosa, "Viscosity of Casting Fluxes Used During Continuous Casting of Steel," <u>Metall. Trans. B,</u> Vol. 12B (2), 1981, pp. 287-298.

23. W.L. McCauley and D. Apelian, "Temperature Dependence of the Viscosity of Liquids," Proceeding of 2nd International Symposium on Metallurgical Slags and Fluxes, 1984, pp. 925-947.

24. P.V. Riboud, Y. Roux, L.D. Lucas, H. Gaye, "Improvement of Continuous Casting Powders," <u>Fachberichte Huttenpraxis Metallweiterverarbeitung,</u> Vol. 19 (8), 1981, pp. 859-869.

25. Y. Meng and B.G. Thomas, "Modeling Interfacial Slag Layer Phenomena in the Shell/Mold Gap in Continuous Casting of Stee," <u>Metall. Mater. Trans. B (USA)</u> (to be submitted), 2002.

26. "MATLAB6.1 Users Manual," The Mathworks, INC, 2001

27. "ANSYS6.1 Users Manual," ANSYS, Inc, 2002

28. K. Schwerdtfeger and H. Sha, "Depth of oscillation marks forming in continuous casting of steel," <u>Metallurgical and Materials Transactions B (USA),</u> Vol. 31B (4), 2000, pp. 813-826B.

29. J. Watzinger and A. Flick, "Online mold friction monitoring system in continuous casting," 84th Steelmaking Conference, (Baltimore, MD, USA), Vol. 84, 2001, pp. 205-213.

30. F. Shahbazian, D. Sichen and S. Seetharaman, "The effect of addition of Al_2O_3 on the viscosity of CaO-'FeO'-SiO_2 -CaF_2 slags," <u>ISIJ Int. (Japan),</u> Vol. 42 (2), 2002, pp. 155-162.

31. Y. Kashiwaya, C.E. Cicutti and A.W. Cramb, "An investigation of the crystallization of a continuous casting mold slag using the single hot thermocouple technique," <u>ISIJ International (Japan),</u> Vol. 38 (4), 1998, pp. 357-365.

32. C. Orrling, S. Sridhar and A.W. Cramb, "In situ observation of the role of alumina particles on the crystallization behavior of slags," <u>ISIJ International (Japan),</u> Vol. 40 (9), 2000, pp. 877-885.

33. M.S. Jenkins and B.G. Thomas, "An Investigation of Some Mold Powder Related Startup Problems," Steelmaking Conference Proceeding 1997, (Chicago, IL, USA), Vol. 80, 1997, pp. 285-293.

Ya Meng and Brian G. Thomas, 2003 ISSTech Steelmaking Conference, Indianapolis, IN, USA, April 27-30, 2003, ISS-AIME, Warrendale, PA, 2003, pp. 589-606.

34. A. Yamauchi, "Heat transfer phenomena and mold flux lubrication in continuous casting of steel," PhD Thesis, Royal Institute of Technology, 2001.

35. H. Nakato, S. Omiya, Y. Habu, K. Hamagami, T. Koshikawa, "Optimizing Mold Lubrication for High-Speed Continuous Casting of Slabs," Journal of metals, Vol. 36 (3), 1984, pp. 44-50.

36. K. Hamagami, K. Sorimachi, M. Kuga, T. Koshikawa, M. Saigusa, "Studies on Quality Improvement in Strand cast Slabs at Chiba Works," Steelmaking Conference, Vol. 65, 1982, pp. 358-364.

37. M. Inagaki, "Improvement Technology of Surface Quality at Velocity Change," CAMP-ISIJ (2), 1989, p. 309.

38. B. Ho, "Characterization of Interfacial Heat Transfer in the Continuous Slab Casting Process," Master Thesis, UIUC, 1992.

39. S. Hiraki, K. Nakajima, T. Murakami, T. Kanazawa, "Influence of mold heat fluxes on longitudinal surface cracks during high speed continuous casting of steel slab," 77th Steelmaking Conference, (Chicago, IL, USA), Vol. 77, 1994, pp. 397-403.